Supporting Information

Nanostructured CuO with a thin g-C$_3$N$_4$ layer as a highly efficient photocathode for solar water splitting

Hyojung Bae[a], Vishal Burungale[b], Wonkyeong Na[b], Hokyun Rho[c], Sang-Wan Ryu[a], Soon Hyung Kang[a], and Jun-Seok Ha[b, *]

Experimental Details

1. Materials

The materials used in the experiment included copper(II) sulfate (anhydrous, Sigma Aldrich), lactic acid (85%, FCC, Sigma Aldrich), and sodium hydroxide (pellets, Sigma Aldrich). Fluorine-doped tin oxide (FTO) coated glass with a surface resistivity of 8 Ω/sq and Cu wire with a diameter of 0.5 mm were purchased from Omniscience and Nilaco, respectively. All chemicals were of analytical grade and were used without purification.
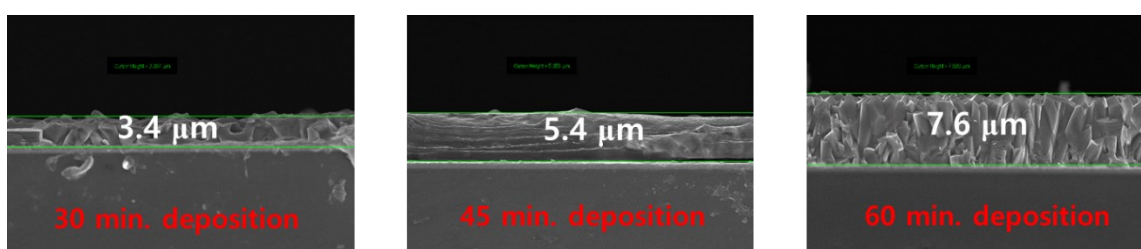
2. Cu₂O electrodeposition

The electrodeposition of Cu₂O occurs as described by the following schematic reaction:

$$2Cu^{2+} + 2e^- + H_2O \rightarrow Cu_2O + 2H^+ \tag{1}$$
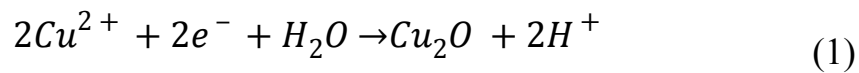
FTO films were cut into pieces with dimensions of 2×2 cm² and were sonicated in acetone, isopropyl alcohol (IPA), and distilled water for 15 min to remove any contaminants from their surfaces. A 0.2 M CuSO₄·5H₂O solution and a 3 M lactic acid solution were freshly prepared with distilled water. The pH values of the solutions were adjusted to just over 11 using NaOH. The experimental setup for Cu₂O electrodeposition consisted of a three-electrode configuration with a Pt wire as the cathode, Ag/AgCl in saturated KCl as the

reference electrode, and an FTO film as the anode. The applied voltage was -0.6 V and the deposition times were 30, 45, and 60 min. The thicknesses of all the Cu$_2$O films were determined using scanning electron microscopy (SEM). Fig. S1 shows that the thickness of Cu$_2$O after 30, 45, and 60 min of deposition were approximately 3.4, 5.4, and 7.6 μm, respectively. Accordingly, the deposition rate

of Cu$_2$O was determined to be ~130 nm/min.

3. Photoelectrochemical (PEC) performance of Cu$_2$O depending on

Fig. S1. Cross-section images of Cu$_2$O electrodeposition with respect to deposition time.
   deposition time

The PEC performance was assessed using a Parstat 4000 potentiostat with a
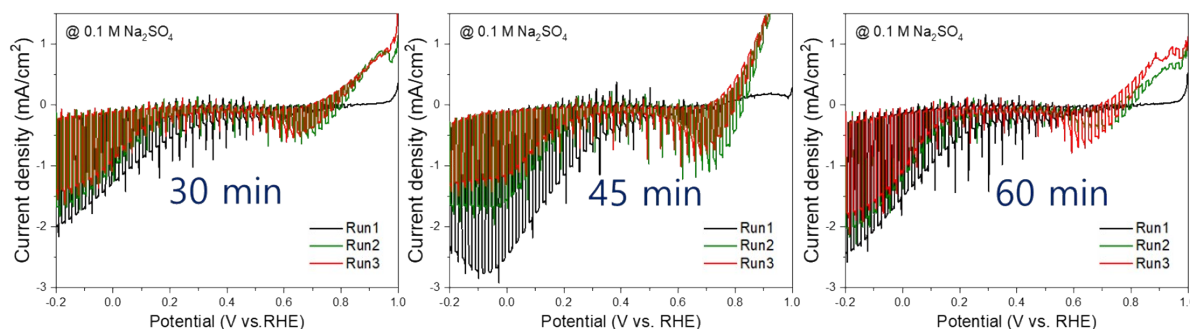

Fig. S2. Linear sweep voltammetry measurements of the Cu$_2$O thin film under chopped illumination with 1-s on/off intervals.

NaOH (1 M) solution as the electrolyte. Fig. S2 shows the chopped photocurrent density of the Cu_2O thin film with respect to the deposition time, where the highest photocurrent density was achieved at 45 min; however, the stability was low. Therefore, considering both efficiency and stability, we chose the Cu_2O thin film prepared with a deposition time of 60 min for our subsequent experiments.

4. Fabrication of the g-C₃N₄/CuO thin film

The optimized Cu_2O thin film was used to fabricate the $g\text{-}C_3N_4/CuO$ thin film. First, 2 g of a urea precursor was dissolved in 10 mL of methanol, and the solution was stirred for 1 h at room temperature. Thereafter, Cu_2O was dipped in the solution for 30 min. The prepared samples were subsequently placed in an oven at 80 °C for 1 h. The samples were then placed in crucibles with covers, which were moved to a muffle furnace for 3 h at 520 °C. After cooling to an ambient temperature, the $g\text{-}C_3N_4/CuO$ thin film was obtained. The process for obtaining CuO was identical to that used to prepare $g\text{-}C_3N_4/CuO$, except the urea

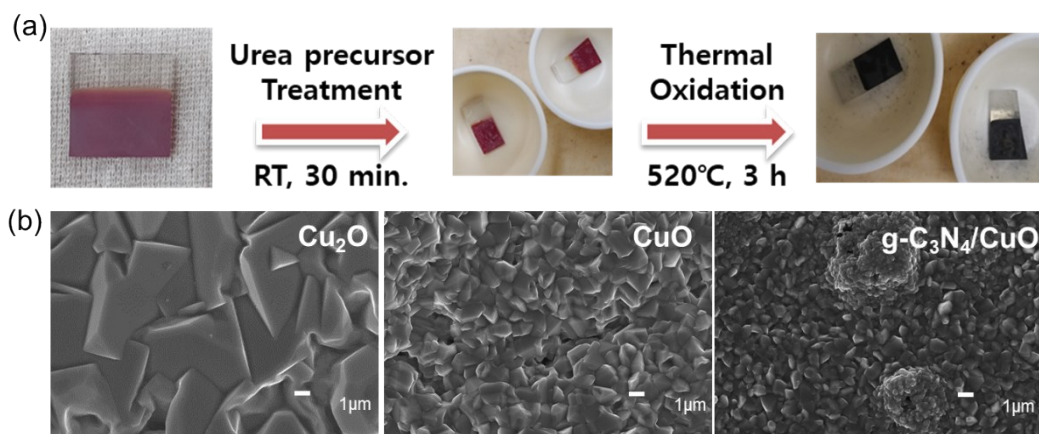Fig. S3. (a) Fabrication procedure and (b) SEM images of CuO and g-C₃N₄/CuO thin films.

precursor treatment was not employed. The fabrication procedure is illustrated in Fig. S3(a).

Before the thermal oxidation stage, Cu_2O was brown. After the Cu_2O film was dipped in the urea–methanol solution, transparent particles formed on its surface. After thermal oxidation, Cu_2O turned into black CuO. The surface morphologies of the resulting Cu_2O, CuO, and g-C_3N_4/CuO thin films were observed using SEM (Fig. S3(b)). The Cu_2O thin film had a larger grain boundary than that of the CuO thin film. Interestingly, unlike CuO, the g-C_3N_4/CuO thin film featured self-assembled regions. These regions were mainly attributed to the use of the urea precursor during thermal oxidation. Moreover, the cross-section SEM images of CuO show that the CuO nanostructure is well formed (Fig. S4).
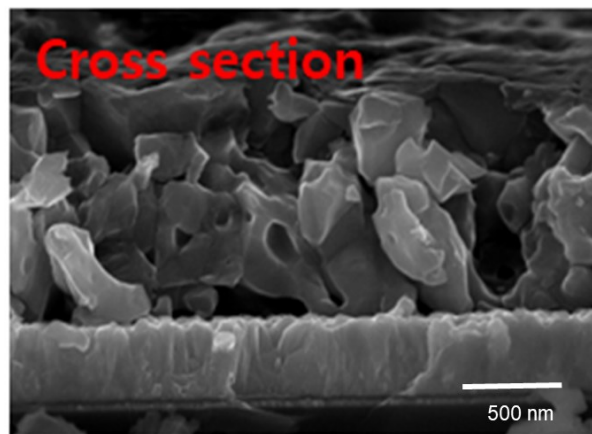
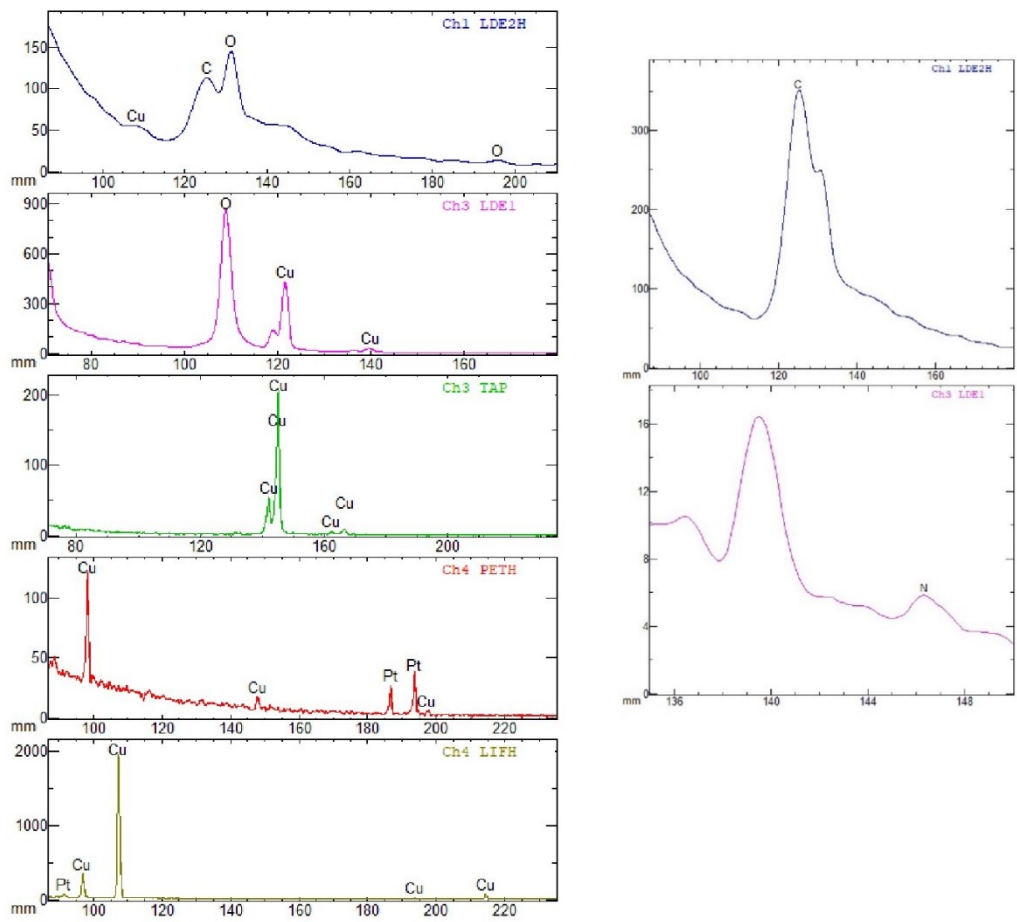

Fig. S4. Cross-section SEM images of the CuO thin film.

Fig. S5. Electron probe X-ray micro analyzer results for the g-C₃N₄/CuO thin film.

5. PEC properties of the g-C$_3$N$_4$/CuO thin film

H$_2$ evolution detection by gas chromatography

The experiments used to detect the hydrogen generated were carried out in a sealed cell, as shown Fig. S6. The working electrode was g-C$_3$N$_4$/CuO and platinum wire was used as the counter electrode. Inert gas (CO$_2$) was continuously flowed through the PEC cell, and a portion of the exiting gas was directed into an Micro GC Fusion (INFICON, Switzerland) with a thermal conductivity detector (TCD) and fast cycling time. The GC-TCD analyses were split into two column, MolSieve 5A and PLOT Q column. The Faradaic efficiency of the CO$_2$ reduction gaseous product is calculated as below;

$$FE\,(\%) = \frac{F \times n_e \times \chi \times F_r}{I}$$

where F is the Faraday constant (96485 C/mol), ne is the number of the electrons required for a hydrogen evolution, x is the mole fraction of the gaseous product obtained from the GC, FCO$_2$ is the molar flow rate of CO$_2$ through the cell, and I is the average current during the run. The faradic efficiency of hydrogen evolution for g-C$_3$N$_4$/CuO photocathode was found to be about 47.35%.
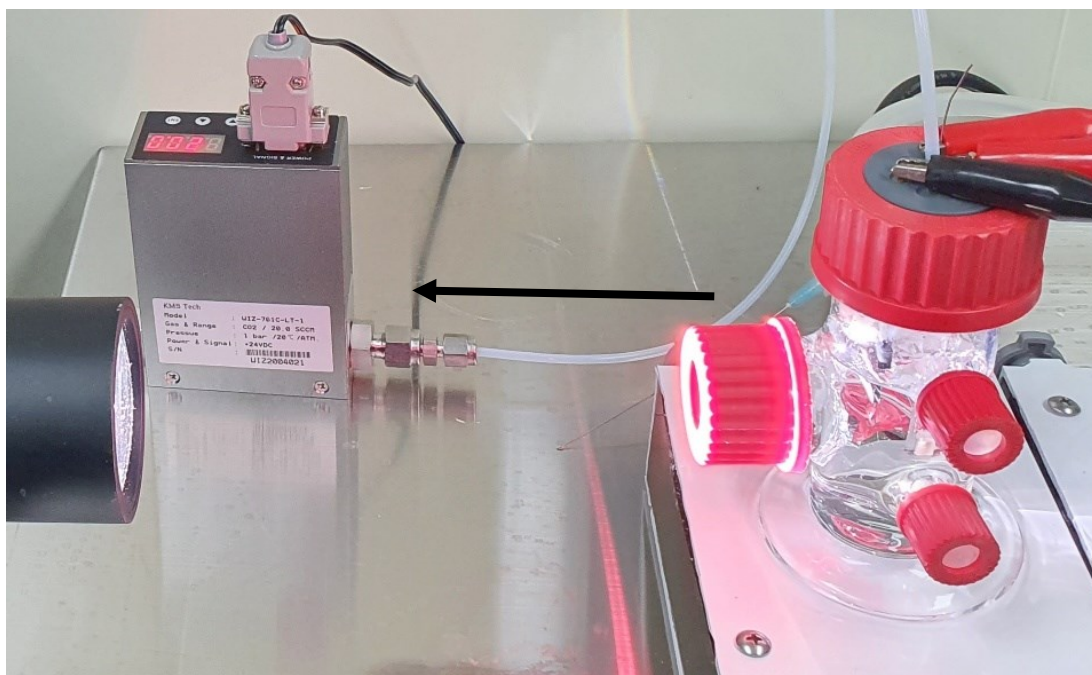

Fig. S6. Experimental setup with Xe lamp for water splitting using g-C$_3$N$_4$/CuO photocathode.

Arrow denote flow direction of CO$_2$ inert gas with flow rate of 20 sccm.